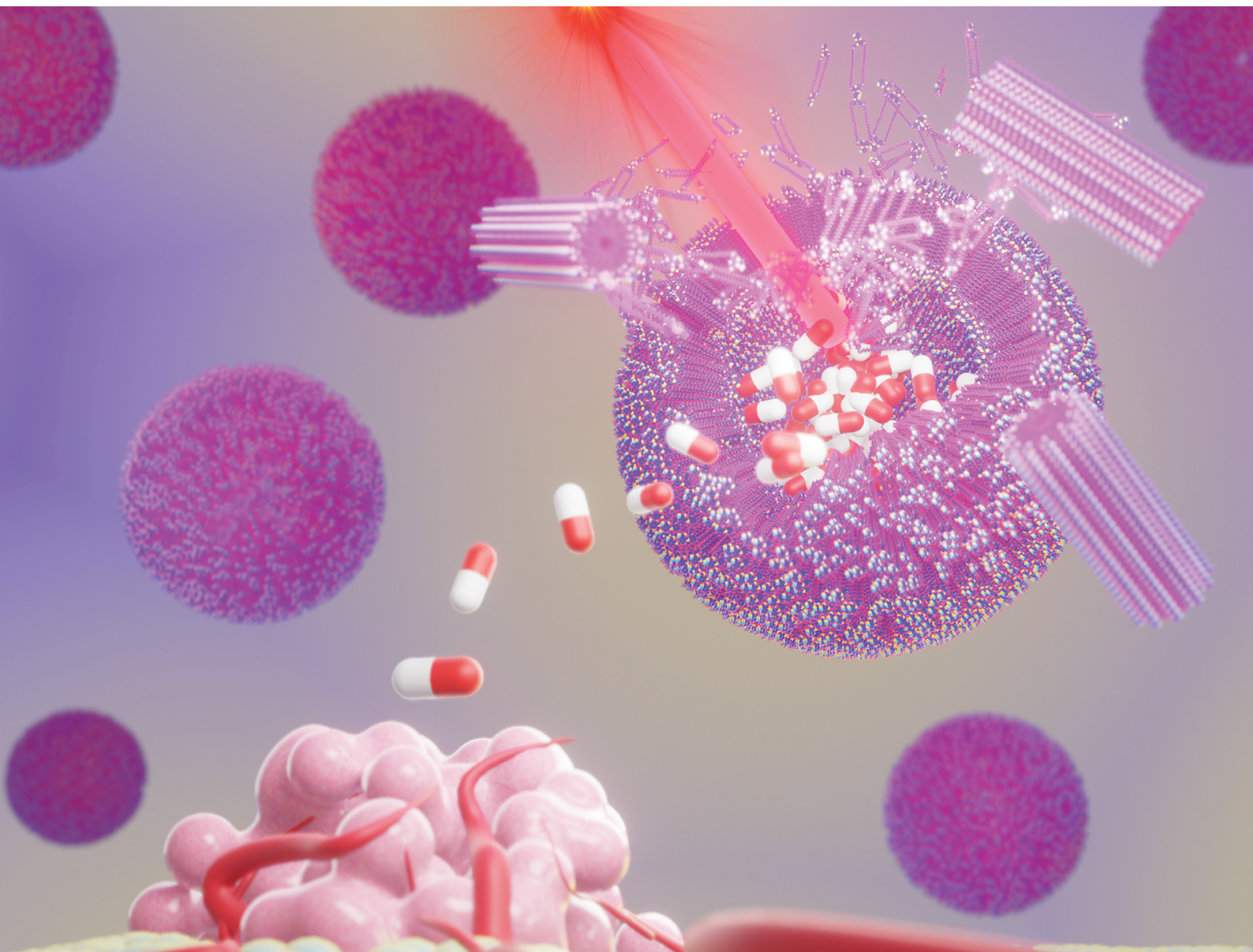


# ChemComm

Chemical Communications

rsc.li/chemcomm



ISSN 1359-7345

**COMMUNICATION**

Debasis Manna *et al.*

Photoresponsive transformation from spherical to nanotubular assemblies: anticancer drug delivery using macrocyclic cationic gemini amphiphiles



Cite this: *Chem. Commun.*, 2021, 57, 4646

Received 18th March 2021,  
Accepted 12th April 2021

DOI: 10.1039/d1cc01468d

rsc.li/chemcomm

# Photoresponsive transformation from spherical to nanotubular assemblies: anticancer drug delivery using macrocyclic cationic gemini amphiphiles†

Subhasis Dey,<sup>a</sup> Soumya Chatterjee,<sup>b</sup> Anjali Patel,<sup>c</sup> Nirmalya Pradhan,<sup>a</sup>  
 Diship Srivastava,<sup>ib</sup> Niladri Patra,<sup>d</sup> Arindam Bhattacharyya<sup>b</sup> and  
 Debasis Manna<sup>ib</sup> \*<sup>ac</sup>

**We developed NIR-light-responsive macrocyclic cationic gemini amphiphiles, one of which displayed various favorable properties of lipids. The NIR-light-mediated cleavage of the strained dioxacycloundecine ring led to the conversion of the spherical to a nanotubular self-assembly in the aqueous medium. This photo-mediated transformation from the spherical to nanotubular self-assembly resulted in the release of encapsulated hydrophobic anticancer drug molecule doxorubicin (Dox) in a controlled manner. The potent cationic gemini amphiphile also displayed lower cytotoxicity and efficient NIR-light-mediated Dox release efficacy to cancerous cells.**

Currently, significant efforts are being dedicated to early diagnosis and developing various biocompatible drug delivery strategies to fight against cancer.<sup>1,2</sup> Lipid-based nanocarriers represent effective agents for efficiently delivering appropriate therapeutic doses of various chemotherapeutic drugs to targeted cancer cells or tissues.<sup>2–5</sup> Besides lower toxicity, biodegradability, prolonged circulation properties, and non-immunogenicity are also the remarkable advantages of lipid-based drug delivery system (DDSs).<sup>6</sup> However, the slow-drug release profiles of various lipid-based DDSs at disease sites significantly compromise their clinical efficiency. It is challenging to control the delivery of appropriate doses of the drug at the right time. Moreover, precisely controlled release of drug molecules into deep tumors is a prerequisite for enhancing the therapeutic efficiency of lipid-based DDSs. Hence, the development of facile methods to synthesize novel lipid-based nanocarriers with excellent drug release profile has been of significant interest.

Cationic lipids have attracted significant attention as efficient DDSs due to the higher abundance of negatively charged phospholipids in the outer membrane of cancer cells.<sup>7,8</sup> Furthermore, if stimuli-responsive linkers are covalently attached to the lipid molecules that can be cleaved following delivery to the cells, this provides a controllable tool for triggering the release of encapsulated drug molecules. The endogenous stimuli are unique for diseased cells or tissue, and they can be exploited for augmenting the specificity of the drug molecules.<sup>6</sup> However, most of the cleavages mediated by these endogenous stimuli are restricted by the limiting conditions obligatory for the release, as they rely on differences in properties between cells. The use of a near-infrared (NIR; exogenous stimulus) light-responsive DDS is one of the attractive strategies as it can be used over long distances with excellent spatial and temporal resolutions.<sup>5</sup> Meanwhile, the poor biocompatibility of several synthetic cationic lipids restricted their clinical applications. Therefore, it is imperative to develop easily synthesizable and biocompatible photo-responsive lipids.

Recently, a photoresponsive lipid–drug conjugate was developed to deliver drug molecules to cancer cells.<sup>9</sup> However, the use of UV-light (365 nm) restricted its further clinical applications.<sup>9</sup> Several liposome-based DDSs were also developed where cocktail mixtures of drug molecules and NIR-light-sensitive dyes were used for NIR-light-mediated drug delivery applications.<sup>3–5,10–13</sup> This approach is time-consuming and an economic burden for both pre-clinical and clinical validation of each molecule associated with the DDSs and the cocktail mixtures of agents. However, the use of only NIR-light-responsive lipids requires the clinical validation of a lower number of molecules.

Most of the reported NIR-light responsive drug carriers are designed with the ester or carbamate moiety as the linker with the photon capturing 2-nitrobenzyl alcohol group. However, the direct attachment of ester, carbamate, and oxime functional groups to the 2-nitrobenzyl moiety makes the linker more susceptible to chemical and enzymatic degradation.<sup>5,12</sup> To

<sup>a</sup> Indian Institute of Technology Guwahati, Chemistry, Guwahati, Assam, India.  
E-mail: dmanna@iitg.ac.in

<sup>b</sup> Calcutta University, Zoology, Kolkata, West Bengal, India

<sup>c</sup> Indian Institute of Technology Guwahati, Centre for the Environment, Guwahati, Assam, India

<sup>d</sup> Indian Institute of Technology (Indian School of Mines) Dhanbad, Chemistry, Dhanbad, Jharkhand, India

† Electronic supplementary information (ESI) available. See DOI: 10.1039/d1cc01468d

curtail the aforementioned problems of structural complexity and linker instability, in this study, we demonstrated the synthesis of 2-nitrobenzyl containing 11-membered strained macrocyclic amphiphiles. We hypothesized that the installation of the UV-active, 2-nitrobenzyl moiety within the highly strained macrocyclic moiety would make it NIR sensitive and endow it with substantial structural change, aggregation behavior, and efficient drug release behavior. Macrocyclic compounds such as calixarenes, cyclodextrins, and others have been used in drug and gene delivery,<sup>14</sup> but NIR-light-responsive macrocyclic amphiphiles have never been applied in drug delivery and represent a comprehensive strategy for smart DDSs. One of the synthesized gemini cationic amphiphile showed successful encapsulation and delivery of the most widely used hydrophobic chemotherapeutic drug Dox to cancer cells.

Modular amphiphiles were synthesized from 3-bromoaniline (Fig. 1A and Scheme S1, ESI<sup>†</sup>). The reductive methylation of 3-bromoaniline provided 3-bromo-*N,N*-dimethylaniline (2). The condensation of 2 with formaldehyde provided 4,4'-methylenebis(3-bromo-*N,N*-dimethylaniline) (3).<sup>15</sup> Subsequent ring-closure reaction *via* Ullmann-type C–O coupling reaction between 3 and (3-nitro-1,2-phenylene)dimethanol (4) resulted in the macrocyclic compound *N*<sup>3</sup>,*N*<sup>3</sup>,*N*<sup>14</sup>,*N*<sup>14</sup>-tetramethyl-7-nitro-6,11-dihydro-17*H*-tribenzo[*c,g,j*][1,6]dioxacycloundecine-3,14-diamine (5). Finally, *N*-alkylation of compound 5 with iodoctane, 1-iodododecane, and 1-iodohexadecane yielded compounds **nIR8**, **nIR12**, and

**nIR16**, respectively. The synthesized macrocyclic compounds are unconventional and structurally quite different from naturally occurring phospholipids.

The hydration of amphiphilic **nIR12** resulted in the spontaneous formation of colloidal aggregates. The hydrophobic effect could be the major driving force for its self-assembly in the aqueous medium. However, the other synthesized amphiphiles failed to self-assemble in the aqueous medium, which could be due to either the high hydration energy (**nIR8**) or the very low hydration energy (**nIR16**). The pyrene-based fluorescence assay revealed that the critical aggregation constant (CAC) of **nIR12** was 28.7  $\mu\text{M}$  (Fig. 1B and Fig. S1, ESI<sup>†</sup>). The lower CAC value suggests the tighter packing of **nIR12** molecules within the spherical NAs, which could be due to the presence of a conformationally restricted cyclic ring in the headgroup region. The field-emission transmission electron microscope (FETEM) analysis revealed the formation of spherical nanoaggregates (NAs) with diameters of 150–200 nm (Fig. 1C). The pH-dependent dynamic light scattering (DLS) measurements showed that the hydrodynamic diameter of **nIR12** varies within 225–275 nm, suggesting its stability in different environments (Fig. S2 and S3, ESI<sup>†</sup>).<sup>8</sup> The smaller hydrodynamic diameter and pH-dependent stability of **nIR12** could be useful for its effective use in clinical applications due to the enhanced permeation and retention (EPR) effect.<sup>6</sup> The surface potential of the NAs was around +13.0 mV at physiological pH, which could be useful for selective targeting of cancer cells over normal cells (Fig. S2, ESI<sup>†</sup>). Meanwhile, the pH-dependent DLS and surface potential measurements of a DPPC/DPPS/**nIR12** (2:2:1) lipid mixture also showed that the hydrodynamic diameter varies within 225–250 nm and the surface potential of the NAs was around +4.8 mV at physiological pH (Fig. S4 and S5, ESI<sup>†</sup>). The higher abundance of PS and other negatively charged lipids makes the outer membrane of cancer cells negatively charged. Therefore, these cationic NAs could show preferential uptake efficiency by cancer cells.<sup>8</sup> The decrease in surface potential with the increase in pH could be due to the increased solvation number.

The temperature-dependent steady-state anisotropy measurements revealed that the phase transition temperature ( $T_m$ ) value of **nIR12** (48  $^{\circ}\text{C}$ ; Fig. 1D) is much higher than that of the dipalmitoylphosphatidylcholine (DPPC) lipid (41  $^{\circ}\text{C}$ ), demonstrating its higher thermal stability and superior drug retention capability at normal body temperature.<sup>8,16</sup> The  $T_m$  value for a mixture of lipids DPPC and dipalmitoylphosphatidylcholine (DPPS) (1:1) was 42  $^{\circ}\text{C}$ . In comparison, the  $T_m$  value for the DPPC/DPPS/**nIR12** (2:2:1) lipid mixture was 47  $^{\circ}\text{C}$  (Fig. S6, ESI<sup>†</sup>). This increase of the  $T_m$  value could be due to the interaction of the cationic ammonium moieties of **nIR12** with the phosphate group of the phospholipids. The lipid mixture also showed excellent liposome formation capability, suggesting the ability of **nIR12** to form liposomes with other model lipids (Fig. S7, ESI<sup>†</sup>), which could be useful in drug delivery, preparing size controllable liposomes, and others. Meanwhile, the molecular dynamics (MD) simulation studies also revealed the formation of a stable lipid bilayer of a mixture of **nIR12**, DOPC, and DOPS and the interaction of the

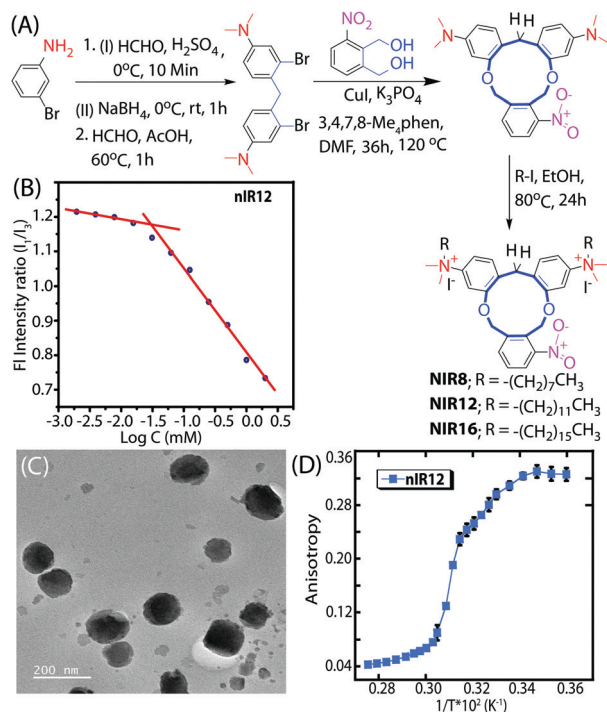


**Fig. 1** Synthetic routes to macrocyclic gemini cationic amphiphiles (A). Measurement of the critical aggregation constant of **nIR12** using a pyrene probe (B). Representative FETEM image of the water-soluble aggregates produced from only **nIR12** (C). The temperature-dependent fluorescence anisotropy measurement of environment-sensitive 1,6-diphenyl-1,3,5-hexatriene dye incorporated within the water soluble aggregates (D).

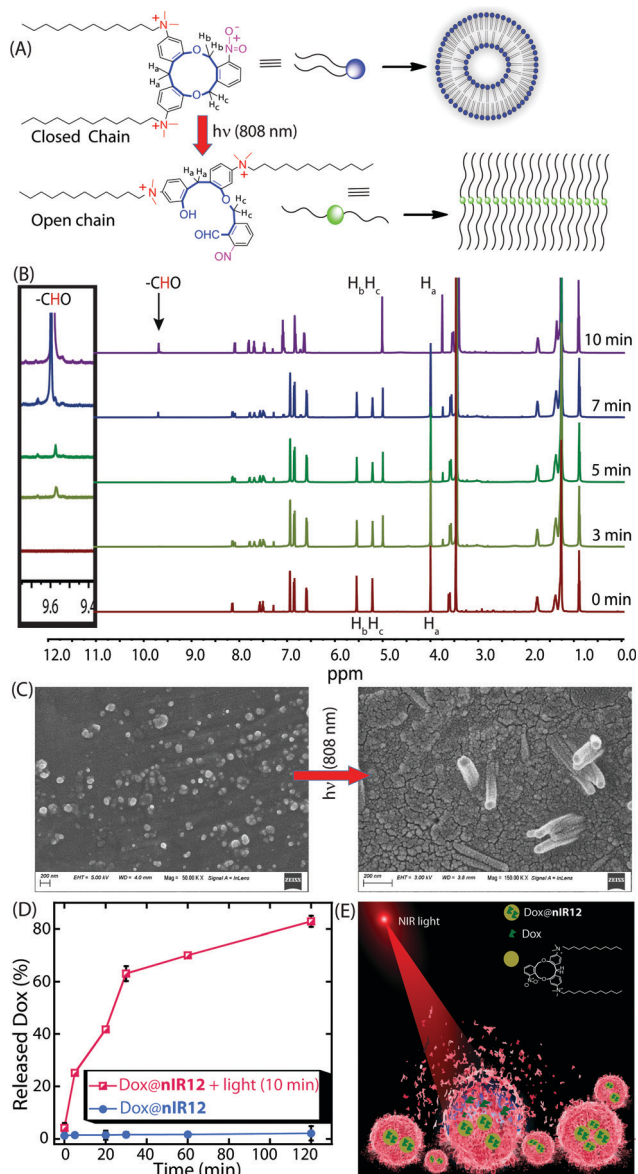


**Fig. 2** The schematic diagram represents the self-aggregation patterns of **nIR12** before and after NIR-light treatment (10 min) (A).  $^1\text{H}$  NMR spectra of **nIR12** without and with NIR-light treatment at different time intervals (B). Representative FESEM images of the water-soluble aggregates produced from only **nIR12** before and after NIR-light treatment (10 min) (C). The Dox release profiles of **nIR12** at pH 7.4 without and with NIR-light treatment (10 min) (D). Cartoon diagram representing the NIR-light treated Dox release from the Dox encapsulated NAs (E).

phosphate groups of the phospholipids with the cationic moieties of **nIR12** (Fig. S8 and Movie S1, ESI $^\dagger$ ).

The NIR-light-mediated ring-opening (Fig. 2A) of macrocyclic amphiphile **nIR12** was confirmed by  $^1\text{H}$  NMR (Fig. 2B). A solution of **nIR12** in  $\text{CDCl}_3$  solvent was irradiated with NIR laser light (808 nm,  $1 \text{ W cm}^{-2}$ ) at different time intervals (0, 3, 5, 7, and 10 minutes). The time-dependent  $^1\text{H}$  NMR analyses revealed the disappearance of characteristic  $H_b$  proton signals (benzyl moiety) at  $\delta = 5.56$  ppm and the appearance of a new signal at  $\delta = 9.69$  ppm that corresponds to the aldehyde proton.

In addition,  $H_a$  ( $\delta = 4.00$  ppm) and  $H_c$  ( $\delta = 5.22$  ppm) proton signals were also shifted to  $\delta = 3.78$  and 5.01 ppm, respectively. Overall, these changes in proton signals in the  $^1\text{H}$  NMR spectra upon photoirradiation indicate the cleavage of the *o*-nitrobenzyl moiety and the opening of the 11-membered strained macrocyclic ring which was further confirmed by mass spectrometric analysis (Fig. S9, ESI $^\dagger$ ). The strained cyclic moiety of **nIR12** is linked with a photon absorbing 2-nitrobenzyl moiety. On NIR-light absorption, the 2-nitrobenzyl group depletes the energy by opening the constrained ring to an open-chain conformation. Within the macrocyclic system, the molecular angular strain leads to a drift from the tetrahedral geometry, which is liable to easy cleavage of the C–O bond *via* the Norrish type II mechanism.<sup>17</sup> The FESEM and FETEM analysis of **nIR12** in the presence of NIR-light also showed a significant change in its aggregation patterns, indicating its instability upon photoirradiation. The spherical aggregation pattern of **nIR12** in the aqueous medium turned into a nanotubular self-assembly (diameter around 3.7 nm) upon NIR irradiation (Fig. 2C and Fig. S8, ESI $^\dagger$ ), which could allow the release of encapsulated drug molecules. The photocleavage of the 2-nitrobenzyl containing macrocyclic ring generated an open-chain conformation, which would self-aggregate in the aqueous medium to form the nanotubular assembly. These organic nanotubes could be beneficial for constructing building blocks for various optoelectronic devices.<sup>18</sup> The FETEM analysis of the DPPC/DPPS/**nIR12** lipid mixture showed complete disruption of the spherical self-assembly after the NIR-light treatment (Fig. S10, ESI $^\dagger$ ). The **nIR12** and DPPC/DPPS/**nIR12** lipid mixture showed adequate loading capability of hydrophobic Dox molecules (41 and 46% at pH 7.4; Fig. S10, ESI $^\dagger$ ) for the chemotherapeutic drug, Dox, suggesting that the hydrophobic Dox molecules could be encapsulated within the hydrophobic core of the spherical assembly of **nIR12**.<sup>8</sup> The Dox release profiles without and with photoirradiation (10 min) showed 2% and 83% release efficiencies after 2 h, respectively (Fig. 2D), suggesting the conformational changes in the presence of NIR-light led to the destabilization of the bilayer assembly of **nIR12** and induced Dox release capability. The Dox release efficiencies from the lipid mixture without and with photoirradiation (10 min) were 2% and 74% after 2 h, respectively (Fig. S11, ESI $^\dagger$ ). This faster Dox release profile of **nIR12** is beneficial for its drug delivery applications, including minimizing adverse effects because of the nonspecific delivery to the healthy cells and augmentation of the local concentration of the Dox molecules within the cancer cells and others (Fig. 2E).

The cell viability assay showed that **nIR12** had a low or negligible toxic effect (after 48 h of incubation) on human MDA-MB-231 (triple-negative breast cancer) cells and human peripheral blood mononuclear cells (PBMCs; healthy cells), indicating its significance in drug delivery applications (Fig. S12, ESI $^\dagger$ ).<sup>16</sup> The MTT assay showed that the  $\text{IC}_{50}$  value of free Dox was  $0.23 \pm 0.02 \mu\text{M}$ . The MTT assay revealed that the  $\text{IC}_{50}$  value of Dox encapsulated **nIR12** (Dox@**nIR12**) with NIR-light treatment (10 min) was  $0.72 \pm 0.05 \mu\text{M}$  (with respect to the effective Dox concentration). However, when the cells were incubated with

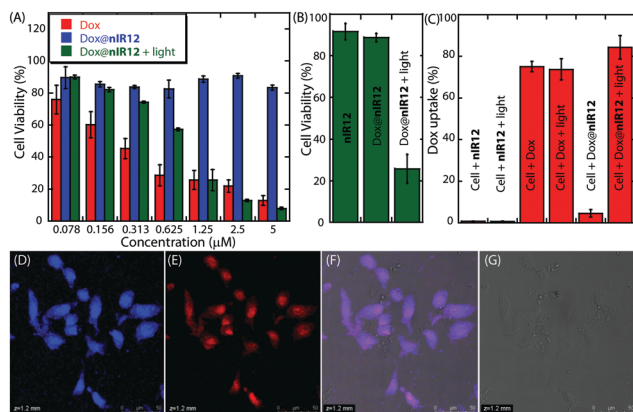


**Fig. 3** Viabilities of MDA-MB-231 cells in the presence of free Dox and Dox@nIR12 after 48 h of incubation (A). Viabilities of MDA-MB-231 cells in the presence of nIR12 (125 µM) and Dox@nIR12 (1.25 µM Dox and 125 µM amphiphile) (B). Flow cytometry analysis to measure the Dox uptake efficiencies of MDA-MB-231 cells treated with nIR12, free Dox (125 µM), and Dox@nIR12 (1.25 µM Dox and 125 µM nIR12) (C). Representative CLSM images of the MDA-MB-231 cells incubated with Dox@nIR12 (1.25 µM Dox and 125 µM amphiphile) for 8 h followed by NIR-light treatment for 10 min. The blue channel (DAPI; D), red channel (Dox; E), overlay of the blue and red channels (F), and bright-field (G) illustrate the Dox release efficacy to MDA-MB-231 cells. Scale bars: 5 µm. The NIR-light (808 nm, 1 W cm<sup>-2</sup>) treatment was done for 10 min.

Dox@nIR12 for 48 h without NIR-light treatment, no significant cytotoxicity was observed (Fig. 3A and B). Hence, the MTT assay results support the successful entrapment and photo-release efficiencies of Dox molecules. Besides, the cellular uptake efficacy of the amphiphile was analyzed by flow cytometry and confocal laser scanning microscopy (CLSM) analyses.<sup>16</sup> The flow cytometry analysis also showed effectual cellular uptake efficiency (Fig. 3C and Fig. S13, ESI<sup>†</sup>). The CLSM images revealed the efficient Dox delivery and release efficacy of nIR12 in the presence of NIR-light (Fig. 3D–G and Fig. S14, ESI<sup>†</sup>). The higher Dox@nIR12 uptake efficiency could be because of the preferable electrostatic interaction of the gemini cationic amphiphile with the negatively charged lipids present in higher abundance on the outer membrane of cancerous MDA-MB-231 cells followed by the endocytosis process. This directed electrostatic interaction could also reduce the side effects of the Dox molecules due to nonspecific delivery.<sup>8</sup> Hence, the higher cellular uptake efficacy of the Dox molecules indicates that this exogenous stimulus significantly controls the drug release efficiency of nIR12.

In conclusion, we developed an *o*-nitrobenzyl containing macrocyclic gemini cationic amphiphile that self-assembles in an aqueous environment to form soluble spherical NAs with favorable properties of DDSs. The NIR-responsive cleavage of the *o*-nitrobenzyl moiety led to the opening of the strained dioxacycloundecine ring to generate a nanotubular self-assembly in the aqueous environment, which could be the driving force for the release of encapsulated drug molecules.

The amphiphile showed lower cytotoxicity and successful entrapment and delivery of the hydrophobic anticancer drug, Dox, to cancerous MDA-MB-231 cells. The NIR-light mediated photocleavage of the amphiphile within the cancer cells promotes cell death. Hence, this simple and innovative concept of developing macrocyclic gemini cationic amphiphiles as potential DDSs could be useful in photodynamic therapy, which could be dissected in a controlled fashion using NIR-light to liberate the enveloped hydrophobic chemotherapeutic drug molecules in a spatially- and temporally-controlled manner for surface and deep-tissue cancer treatment.

The authors acknowledge the Department of Biotechnology, Government of India (BT/PR41335/NNT/28/1780/2021), for financial support. NP acknowledges TEQIP-III for funding.

## Conflicts of interest

There are no conflicts to declare.

## References

- B. Li, Z. Yuan, P. Zhang, A. Sinclair, P. Jain, K. Wu, C. Tsao, J. Xie, H. C. Hung, X. Lin, T. Bai and S. Jiang, *Adv. Mater.*, 2018, **30**, e1705728.
- M. J. Mitchell, M. M. Billingsley, R. M. Haley, M. E. Wechsler, N. A. Peppas and R. Langer, *Nat. Rev. Drug Discovery*, 2021, **20**, 101–124.
- J. M. Chen, T. J. Fan, Z. J. Xie, Q. Q. Zeng, P. Xue, T. T. Zheng, Y. Chen, X. L. Luo and H. Zhang, *Biomaterials*, 2020, **237**, 119827.
- A. Raza, U. Hayat, T. Rasheed, M. Bilal and H. M. N. Iqbal, *J. Mater. Res. Technol.*, 2019, **8**, 1497–1509.
- Y. Tao, H. F. Chan, B. Y. Shi, M. Q. Li and K. W. Leong, *Adv. Funct. Mater.*, 2020, **30**, 1–28.
- H. S. El-Sawy, A. M. Al-Abd, T. A. Ahmed, K. M. El-Say and V. P. Torchilin, *ACS Nano*, 2018, **12**, 10636–10664.
- R. B. Birge, S. Boeltz, S. Kumar, J. Carlson, J. Wanderley, D. Calianese, M. Barcinski, R. A. Brekken, X. Huang, J. T. Hutchins, B. Freimark, C. Empig, J. Mercer, A. J. Schroit, G. Schett and M. Herrmann, *Cell Death Differ.*, 2016, **23**, 962–978.
- S. Dey, A. Patel, K. Raina, N. Pradhan, O. Biswas, R. Thummer and D. Manna, *Chem. Commun.*, 2020, **56**, 1661–1664.
- S. Alam, D. S. Alves, S. A. Whitehead, A. M. Bayer, C. D. McNitt, V. V. Popik, F. N. Barrera and M. D. Best, *Biocorjugate Chem.*, 2015, **26**, 1021–1031.
- F. Wang, Z. W. Yuan, P. McMullen, R. X. Li, J. R. Zheng, Y. Xu, M. J. Xu, Q. He, B. W. Li and H. Y. Chen, *Chem. Mater.*, 2019, **31**, 3948–3956.
- Y. W. Sun, Y. Y. Ji, H. Y. Yu, D. Wang, M. W. Cao and J. Q. Wang, *RSC Adv.*, 2016, **6**, 81245–81249.
- R. Weinstein, T. Slanina, D. Kand and P. Klan, *Chem. Rev.*, 2020, **120**, 13135–13272.
- J. Xiang, X. Tong, F. Shi, Q. Yan, B. Yu and Y. Zhao, *J. Mater. Chem. B*, 2018, **6**, 3531–3540.
- J. J. Yu, D. W. Qi and J. W. Li, *Commun. Chem.*, 2020, **3**, 189.
- T. Pastierik, P. Sebej, J. Medalova, P. Stacko and P. Klan, *J. Org. Chem.*, 2014, **79**, 3374–3382.
- A. Saha, S. Panda, S. Paul and D. Manna, *Chem. Commun.*, 2016, **52**, 9438–9441.
- M. Oelgemoeller and N. Hoffmann, *Org. Biomol. Chem.*, 2016, **14**, 7392–7442.
- Y. J. Huang, Z. R. Wang, Z. Chen and Q. C. Zhang, *Angew. Chem., Int. Ed.*, 2019, **58**, 9696–9711.